

# Eigenhill vs. Eigenface and Eigenedge

Alper YILMAZ

Muhittin GÖKMEN

Istanbul Technical University

Department of Computer Science

yilmaz@cs.ucf.edu

gokmen@cs.itu.edu.tr

## Abstract

*In this study, we present a new approach to overcome the problems in face recognition associated with illumination changes by utilizing the edge images rather than intensity values. However, using edges directly has its problems. To combine the advantages of algorithms based on shading and edges while overcoming their drawbacks, we introduced “hills” which are obtained by covering edges with a membrane. Each hill image is then described as a combination of most descriptive eigenvectors, called “eigenhills”, spanning hills space.*

*We compare the recognition performances of eigenface, eigenedge and eigenhills methods by considering illumination and orientation changes on Purdue A&R face database and showed experimentally that our approach has the best recognition performance.*

## 1. Introduction

Face recognition is one of the leading research topics among researchers. Researchers focused on recognition of faces in strictly controlled environments. Yuille et. al [1] tried to obtain subjective features by template matching, while others tried to obtain the variation among images for classification purposes. One of the important studies on describing the changes in face classes, “eigenfaces for recognition”, was proposed by Pentland and Turk [2], which depended on characterizing the information of each subject face in a low dimensional feature space by using Karhunen-Loeve expansion (KLT).

Though, eigenfaces boost the researches on recognition of faces, the idea itself is prone changes in illumination. Studies to solve the illumination problem focused on modeling of illumination effect on faces or finding illumination free features to describe a face. Takacs and Wechsler proposed an edge based approach to recognize faces using Hausdorff distance [4]. Belhumeur et. al. [5]

developed fischerface approach to overcome the illumination changes.

In this study, we proposed an algorithm based on KLT to overcome problems due to illumination variation and pose changes. Our approach depends on the fact that edges do not change considerably in varying illumination. However, edges bring their own problems, they are very sensitive to pose and orientation changes of the face. We overcome these problems by covering the edges with a membrane, which is related to regularization theory.

The organization of this paper is as follows. In the next section, a theoretical analysis of illumination effect on gray scales and edge maps is given. In the following section, we give brief descriptions of the eigenface, edge-based approach and our method, the eigenhill. Then, performances of three methods on Purdue face database are examined. In last section, a conclusion is given.

## 2. Illumination Effect on Face and Edges

For two point light sources, one is on at a particular time, illumination change can alter the appearances of objects. To describe effect of illumination variation, we will identify the differences of two lighting patterns of an object for two distinct light sources. In the case of a lambertian surface, the image is determined by the image irradiance equation,  $I(x,y)=R(p,q,p_s,q_s)$ , where

$$R(p,q;p_s,q_s) = \frac{1 + pp_s + qq_s}{\sqrt{1 + p_s^2 + q_s^2} \sqrt{1 + p^2 + q^2}} \quad (1)$$

and  $p = \partial z / \partial x$ ,  $q = \partial z / \partial y$ , while  $z$  is the depth map of the object. For two different light sources  $(p_{s1}, q_{s1})$  and  $(p_{s2}, q_{s2})$ , where  $p_{s2} = p_{s1} + \delta_{ps}$  and  $q_{s2} = q_{s1} + \delta_{qs}$ , corresponding reflectance maps will be,

$$R_i(p,q;p_{s_i},q_{s_i}) = \frac{1 + pp_{s_i} + qq_{s_i}}{\sqrt{A} \sqrt{1 + p^2 + q^2}} \quad (2)$$

$$R_2(p, q, p_{s_1}, q_{s_2}) = \frac{1 + pp_{s_1} + qq_{s_2} + p\delta_{ps} + q\delta_{qs}}{\sqrt{B}\sqrt{1+p^2+q^2}} \quad (3)$$

where, for  $\delta_{ps} \neq 0$ ,  $\delta_{qs} \neq 0$ ,  $A$  and  $B$  is given by,

$$A = 1 + p_{s_1}^2 + q_{s_1}^2 \quad (4)$$

$$B = 1 + p_{s_1}^2 + q_{s_1}^2 + 2p_{s_1}\delta_{ps} + 2q_{s_1}\delta_{qs} + \delta_{ps}^2 + \delta_{qs}^2. \quad (5)$$

The edge of objects can be obtained via zero crossings of laplacian operator,  $\nabla^2 R = R_{xx} + R_{yy}$ , where  $R_{xx}$  and  $R_{yy}$  represent second derivatives of  $R$  with respect to  $x$  and  $y$ .

In the following sub-sections, analysis of changes between edges and textures of objects for four cases, planar objects, spheres and simulated and real faces, is given.

### 2.1. Planar Object

In planar lambertian surfaces, the depth,  $z$ , does not change. Thus,  $p = z_x = 0$ ,  $q = z_y = 0$  and the image is seen equally bright in all directions. The reflectance map corresponding to planar case is,  $R(p_s, q_s) = 1/\sqrt{1+p_s^2+q_s^2}$ . The laplacian of the  $R(p_s, q_s)$  is,  $\nabla^2 R = R_{xx} + R_{yy} = 0 + 0 = 0$ , thus the planar case does not have any edges except on the boundaries, and two edge maps obtained for two different illumination will be the same.

On the other hand, the difference of gray levels between two images of the same planar surface is,

$$|R_1 - R_2| = \left| \frac{\sqrt{B} - \sqrt{A}}{r\sqrt{B}\sqrt{A}} \right| \quad (6)$$

and  $\sqrt{B} - \sqrt{A} \neq 0$ . Thus, we have  $|\nabla^2 R_1 - \nabla^2 R_2| < |R_1 - R_2|$ , thus for planar surfaces edges are more robust representations.

### 2.2. Spherical Object

For spherical lambertian objects, the depth information is  $z^2 = r^2 - x^2 - y^2$ , where  $r$  is the radius of the sphere. Let's assume  $C = r^2 - x^2 - y^2$ . Thus  $R$  will be,

$$R(p, q; p_s, q_s) = \frac{\sqrt{C} - xp_s - yq_s}{r\sqrt{A}} \quad (7)$$

Laplacian of this reflectance map can be obtained as,

$$\nabla^2 R = x^2 + y^2 - 2r^2 / r\sqrt{A}\sqrt{C}^3. \quad (8)$$

Zero crossings of  $\nabla^2 R$  will occur only when  $x^2 + y^2 = 2r^2$ , which are the boundary locations of the sphere. Hence, the difference between edge maps is,  $|\nabla^2 R_1 - \nabla^2 R_2| = 0$ . On the other hand, the difference between intensity values is,

$$|R_1 - R_2| = \left| \frac{(\sqrt{C} - xp_{s_1} - yq_{s_1})}{r\sqrt{A}\sqrt{B}} (\sqrt{B} - \sqrt{A}) + \frac{x\delta_{ps} + y\delta_{qs}}{r\sqrt{B}} \right| \quad (9)$$

If we take limit of  $|R_1 - R_2|$  as  $\delta_{ps}$ ,  $\delta_{qs}$  go to infinity we get,

$$\lim_{\delta_{ps}, \delta_{qs} \rightarrow \infty} |R_1 - R_2| = \infty \quad (10)$$

This reveals that  $|\nabla^2 R_1 - \nabla^2 R_2| \leq |R_1 - R_2|$  for the spherical lambertian objects.

### 2.3. Simulated Faces

As compared to above situations, human faces have highly non-convex shape creating cast shadows. In order to observe the importance of non-convex structure on edges, we constructed experiments on a wire-frame faces. To utilize effects of varying illumination, point light sources are located in a semi-circle with  $22.5^\circ$  apart. We placed an ambient light source to simulate natural lighting conditions. Rendered faces from wire-frame structure by turning on one light source at a time along with the ambient light are shown in Fig.1.a and corresponding edge maps are shown in Fig.1.b.

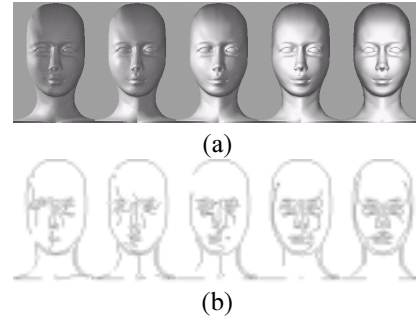


**Figure 1.** (a) Rendered faces with one point light source along with the ambient light source, (b) corresponding edge maps.

To quantitatively evaluate the effect of variation in illumination for simulated faces, we used the probabilistic measures,  $\Pr(\text{IE}|\text{DE})$ ,  $\Pr(\text{DE}|\text{IE})$  and mean square distance (MSD), where IE is ideal edge and DE is detected edge. MSD of detected edges from ideal edges is calculated as 4 pixels. The probabilities are calculated for  $7 \times 7$  masks in order to compensate the movements of narrow-structured edges. This indicates that edges cannot be directly utilized for a robust face recognition scheme, their narrow structure should be widened. However, this modification should not disturb the localization of the edge point.

## 2.4. Real Face Images

After simulation experiments, we scrutinized the case for real world faces of Purdue A&R face database. We used the natural lighting conditions of 113 subject faces as the ideal set and three groups of 339 images as the test set, containing faces illuminated with left, right and both left and right light sources. The three groups and the ideal face and edges associated with them are shown in Fig.2.



**Figure 2.** First row ideal face (leftmost) and test faces. Second row corresponding edges.

Afore-mentioned probabilistic calculations for quantitative evaluations are plotted in Fig.3 for 1x1 and 7x7 neighborhood masks. The use of 7x7 mask is due to non-ideal alignment of camera in addition to the reasons stated in the previous section.

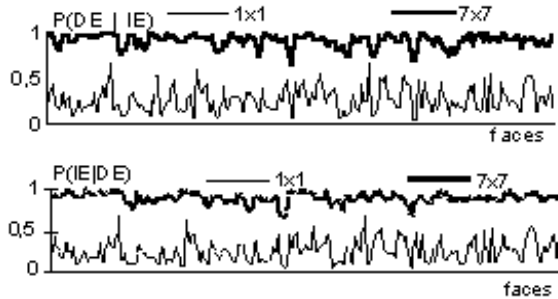


**Figure 3.** Probabilistic measures,  $\Pr(IE|DE)$  and  $\Pr(DE|IE)$  for 1x1 and 7x7 masks.

## 3. Methods

Given a set of faces, the classification of faces can be achieved in a low dimensional space rather than using a high dimensional face space. Low dimensional space can be found by KLT, which is capable of reconstructing original face from unlabelled faces, since it holds adequate information of variations for each face of the learning set.

In this section, we will give a brief description of eigenface scheme along with an edge based KLT scheme, and our approach, the eigenhill scheme.

## 3.1. Eigenfaces

Eigenface method is based on dimensionality reduction obtained by KLT [2]. The new dimensions are defined to decrease the correlation among  $T$  faces constructing the learning set. In KLT, orthonormal eigenvectors,  $u_i$  and eigenvalues,  $\lambda_i$ , of the covariance matrix,  $C$ , calculated from face vectors are used to obtain low dimensional representation, where  $i=1, \dots, T-1$ . Since the variation can be formulated by selecting  $M$  maximum eigenvalued eigenvectors (eigenfaces), where  $M < T$  [2], each face can be reconstruct by weighted,  $w_i$  for  $i=1, \dots, M$ , sum of eigenvectors. The characteristic  $W_j$  vector which is used as reduced face space of  $j^{\text{th}}$  face class,  $j=1, \dots, T$ , is formed by  $w_i$  weights and nearest neighbor classifier in the reduced feature space performs the recognition.

There are two basic drawbacks of this approach. First one is, a change in illumination will degrade the recognition performance. Second one is the presence of noise in the subject image. These performance degradations are due to the fact that eigenface method is highly sensitive to local texture information within a face.

Instead of using highly variable local information, more robust descriptive property can be used. Edge maps are important features which are not distorted by illumination changes as shown in the previous section.

## 3.2. Edge based Eigenspace Decomposition

To utilize the advantages of edges, 2D Generalized Edge Detector (GED) [6], which unifies most of the well-known edge operators, such as Canny, Deriche, etc., under a framework, is used. GED represents edge maps in  $\lambda\tau$  space, which is an extension to the scale space representation. It is based on regularization theory, which utilizes convex combination of membrane and thin plate energy functionals.

Eigenspace decomposition can be applied to edge maps of the learning set. In this case eigenvectors is be named "eigenedges".

A drawback of eigenedge approach is the locality of edge representation. Any change in facial expression or a shift in edge locations due to small rotation of the edges will result in recognition performance degradation. On the other hand, if the images are taken in strictly controlled manner, eigenedge system gives acceptable performance.

However, it is not guaranteed to attain strict control on the orientation and expression of face.

### 3.3. Eigenhills

To overcome the locality problem of edges, a membrane functional,

$$E_m(f, \lambda) = \iint_{\Omega} (f-d)^2 dx dy + \lambda(1-\tau) \iint_{\Omega} (f_x^2 + f_y^2) dx dy \quad (11)$$

can be applied to edge maps. The spread edge profiles obtained by a membrane, composes a ghostly face, “hill”. Hills have high values on boundary locations and decrease as we move apart from edges. Hills are shown in Fig.4b.

It is known that, minimizing the membrane functional is equivalent to convoluting the data with a first order regularization filter,  $R_1(x, y; \lambda)$ , [6],

$$R_1(x, y; \lambda) = (1/2\lambda) e^{-((|x|+|y|)/\lambda)} \quad (12)$$

which is shown in Fig.4a.



Figure 4. (a) R1 filter ( $\lambda=2$ ), (b) Sample hills.



Figure 5. Eigenhills.

Low dimensional representations of hills can be determined by KLT. Eigenvectors of covariance matrix defined for hills is named as “eigenhills”, and they are shown in Fig.5.

## 4. Results and Conclusion

To show that eigenhills approach is more robust to illumination changes compared to eigenface and edgedge, we used simulated and real face images by utilizing two criteria: recognition measure,  $\mathcal{E} = \|W_l - W_t\|_2$ , where  $l$  is learning and  $t$  is test set, and reconstruction error,  $\mathcal{E} = \|\Gamma^r - \Gamma_l\|_2$ , where  $\Gamma^r$  is reconstructed face.

### 4.1. Simulated faces

In the experiments, we used the learning set of Fig.6 along with the test set of Fig.1a. Since the simulated faces are designed on strictly controlled environment, there is no

non-ideal alignment of edges, so performance comparison would be made only on varying illumination.



Figure 6. Learning set constructed using Maya®.

The comparison for the faces is acquired by measuring the distance of the reconstructed face/hill to the recognized face in the face/hill space. Resulting diagrams for face space distance and weight distance are given in Fig.7a and b respectively. In diagrams distances indicates that eigenhills has better performance than the eigenfaces.

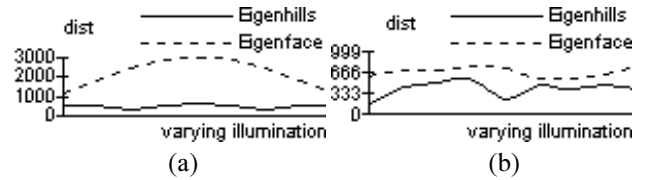


Figure 7. Distance of reconstructed face to (a) face space, (b) weight space.

### 4.2. Real faces

To observe the performance of real face images, we tested three approaches on 126 individuals of Purdue face database [7]. In experiments, we used natural lighting conditions as learning set, Fig.8a, test set of 756 faces of six categories: left side light is on, right side source is on, both sidelights are on, and three facial expressions, angry, laughing and screaming, shown in Fig.8b.



Figure 8. (a) Learning set, (b) test set faces.

Average reconstruction distances given in Table 1 confirms that eigenhill has better performance compared to edgedges, and eigenfaces. Edgedges gave the poorest performance due to non-ideal alignment and low correlation among edge maps.

Table 1. Average distance to face space.

	Both sidelight	Left sidelight	Right sidelight	Scream	Laugh	Anger
Eigenface	300	167	219	<b>131</b>	<b>80</b>	<b>98</b>
Eigenedge	250	252	250	258	236	252
Eigenhill	<b>151</b>	<b>108</b>	<b>120</b>	140	86	109

Recognition performances for the three systems are given in Table 2. From the table it is observed that the recognition performance for all three lighting conditions for eigenhills is 86.4%, while for eigenface it is only 69.8%. Eigenedge method has the poorest recognition performance. Recognition performance of eigenhills for facial expression change is 88.8%, which is above eigenface's performance, 88.4%.

**Table 2.** Recognition performances.

	Both sidelight	Left sidelight	Right sidelight	Scream	Laugh	Anger
Eigenface	44.7%	85.8%	79.1%	<b>83.8%</b>	92.9%	89.1%
Eigenedge	18.7%	34.2%	27.5%	16.7%	42.5%	30.0%
Eigenhill	<b>80.2%</b>	<b>91.6%</b>	<b>87.5%</b>	79.8%	<b>95.0%</b>	<b>91.6%</b>

Note that, overall recognition performance of eigenhill is 89.4%, which is above eigenface's overall recognition performance, 82.3%. Also, overall performance of the eigenedge method 38.8%, is below the acceptable range.

From the results of the experiments given above, we conclude that eigenhills approach is more robust to illumination variation than eigenface and eigenedge.

## 5. References

- [1] A.L. Yuille, D.S. Cohen, and P.W. Hallinan, "Feature extraction from faces using deformable templates", Proc. of CVPR, San Diego, CA. June 1989.
- [2] M. Turk, A. Pentland, "Eigenfaces for recognition", Journal of Cognitive Sciences Vol.3 Num.1, 1991, pp71-86.
- [3] S.K. Nayar, H. Murase, S.A. Nene, "Parametric appearance representation," from Early Visual Learning, Oxford University Press 1996, pp131-160.
- [4] B. Tàcacs and H. Wescler, "Face recognition using binary image metrics," Proc. of the 3rd Int. Conf. on Automatic Face and Gesture Recognition, Nara, Japan, April 1998, pp294-299.
- [5] P.N. Belhumeur, J.P. Hespanha and D.J. Kriegman, "Eigenfaces vs. Fischerfaces: Recognition Using Class Specific Linear Projection," IEEE PAMI, Vol. 19, No. 7, July 1997.
- [6] B. Kurt, M. Gökmen, "2D Generalized edge detector", Proc. of National IEEE Conf. on Signal Processing and Applications, Bilkent, Ankara, Turkey, June 1999.
- [7] Purdue Face Database, [www.purdue.edu/](http://www.purdue.edu/)